Bacterial community response to species overrepresentation or omission is strongly influenced by life in spatially structured habitats

Kleyer, Hannah[1], Tecon, Robin[1,2] and Or, Dani[1,3]

[1]Soil and Terrestrial Environmental Physics, Department of Environmental Systems Science, Swiss Federal Institute of Technology in Zurich (ETH Zürich), Universitätstrasse 16, 8092 Zürich, Switzerland

[2]National Centre of Competence in Research (NCCR) Microbiomes, University of Lausanne, Biophore Building, 1015 Lausanne, Switzerland

[3]Division of Hydrologic Sciences, Desert Research Institute, Reno, NV, USA

Running title: Habitat structure affects bacterial assembly

Keywords: bacterial interactions, absolute quantification, real-time PCR, fluidigm, porous media

Abstract

Variations in type and strength of interspecific interactions in natural bacterial communities (e.g., synergistic to inhibitory) affect species composition and community functioning. The extent of interspecific interactions is often modulated by environmental factors that constrain diffusion pathways and cell mobility and limit community spatial arrangement. We studied how spatially structured habitats affect interspecific interactions and influence the resulting bacterial community composition. We used a bacterial community made of 11 well-characterized species that grew in porous habitats (comprised of glass beads) under controlled hydration conditions or in liquid habitats. We manipulated the initial community composition by overrepresenting or removing selected members, and observed community composition over time. Life in porous media reduced the number and strength of interspecific interactions compared to mixed liquid culture, likely due to spatial niche partitioning in porous habitats. The community converged to similar species composition irrespective of the initial species mix, however, the dominant bacterial species was markedly different between liquid culture and structured porous habitats. Moreover, differences in water saturation levels of the porous medium affected community assembly highlighting the need to account for habitat structure and physical conditions to better understand and interpret assembly of bacterial communities. We point at the modulation of bacterial interactions due to spatial structuring as a potential mechanism for promoting community stability and species coexistence, as observed in various natural environments such as soil or human gut.

Importance

Bacteria live as complex multispecies communities essential for healthy and functioning ecosystems ranging from soil to the human gut. The bacterial species that form these communities can have positive or negative impact on each other, promoting or inhibiting each other's growth. Yet, the factors controlling the balance of such interactions in nature, and how these influence the community, are not fully understood. Here, we show that bacterial interactions are modified by life in spatially structured bacterial habitats. These conditions exert important control over the resulting bacterial community regardless of initial species composition. The study demonstrates limitations of inferences from bacterial communities grown in liquid culture relative to behaviour in structured natural habitats such as soil.

Introduction

Advances in high-throughput sequencing uncovered vast diversity of microbiomes present in all ecosystems: from soils (Bahram et al 2018, Delgado-Baquerizo et al 2018) and oceans (Ibarbalz et al 2019), to plants and animals (Bai et al 2015), to humans (Costea et al 2018) and urban habitats (Afshinnekoo et al 2015). The important roles that microorganisms play in ecosystem functioning and health have prompted interest in better understanding microbial assembly, stability and activity, towards improved prediction and control of community formation and function (Lawson et al 2019, Widder et al 2016). Resolving the mechanisms that support coexistence of diverse species within a shared environment is particularly challenging, as are the balance of interactions within multispecies assemblages (Little et al 2008) and how such interactions are influenced by habitat characteristics.

Simple experimental ecosystems yield new insights through systematic hypotheses testing and controlled evaluation of theoretical concepts (Cairns et al 2018, Carlström et al 2019, Chodkowski and Shade 2017, Friedman et al 2017, Meroz et al. 2021, Kehe et al 2019, Voges et al 2019). Such approaches have confirmed several essential drivers of community assembly and species interactions, notably the nature and availability of nutrient and carbon resources (Enke et al 2019, Fu et al. 2020, Goldford et al 2018), population density(Abreu et al 2019), rates of migration (Gokhale et al 2018), and how environmental toxicity affects functionality(Piccardi et al 2019). The role of microbial habitat spatial structure has received comparatively less attention, despite well-established understanding in ecological theory that spatially structured environments influence biodiversity, interactions and species coexistence (Nadell et al 2016, Tilman 1994). A few experimental and modelling studies have shown that microhabitat spatial structure could stabilize simple assemblages of 2-3 bacterial species that would not coexist in mixed cultures due to competitive exclusion (Borer et al 2018, Kim et al 2008, Lowery and Ursell 2019, Wang and Or 2013). Therefore, spatial habitat heterogeneity

affects bacterial community dynamics in ways irreproducible in homogeneous (liquid) habitats. Here, we hypothesize that spatially structured habitats, such as found in soil and other porous media, dominate the nature of bacterial interactions in space and thus exert a significant influence on bacterial community dynamics. More specifically, porous domains that are partially water-saturated constrain nutrient fluxes and interspecies competition thus providing specific life conditions different from well-mixed habitats (Ebrahimi and Or 2015, Tecon et al 2018, Wang and Or 2013). To test this hypothesis, we have used a simplified bacterial community of 11 species (Kleyer et al 2019) in replicate microcosms supplied with the same nutrient resources but with variation in spatial structure and hydration state (Fig. 1). The porous habitats comprised of glass beads were set at controlled hydration states from wet to relatively dry, while liquid media without beads served as contrasting unstructured habitats. The synthetic community comprises 11 members from phyla commonly found in soil (*Proteobacteria, Actinobacteria* and *Firmicutes*). Functional traits with relevance for the soil environment include decomposition of organic matter, nutrient cycling, and maintenance of soil fertility. In particular, the community members play an important role in nitrogen fixation (*Paenibacillus sabinae, Pseudomonas stutzeri*, *Rhizobium etli*, *Xanthobacter autotrophicus*), are involved in bioremediation of different components like phenols (*Arthrobacter chlorophenolicus* (Westerberg et al 2000)), polychlorinated biphenyl (PCB) (*Burkholderia xenovorans* (Liang et al 2014)), polycyclic aromatic hydrocarbons (PAHs) (*Pseudomonas stutzeri* (Singh et al 2017)) and halogenated hydrocarbons (*Xanthobacter autotrophicus*). We added *Escherichia coli* as non-soilborne species to the community as *E. coli* often ends up in the environment as faecal contaminant (Brennan et al 2010). All members can grow aerobically and some are able to enter dormancy by forming spores (*Bacillus subtilis, Paenibacillus sabinae,* and *Streptomyces violaceoruber* (Brenneret al (2005)). Thus, the selected synthetic community covers a wide phylogenetic range and combines bacterial species with different life strategies. To uncover interactions within this community, we manipulated the initial composition of the inoculum by

100 systematically over representing one species at a time. Our working hypothesis was that
101 spatially structured habitats would select for a bacterial community composition that differs
102 from liquid culture habitats, moreover, we predicted that the resulting community composition
103 in structured habitats would be marginally affected by the initial inoculum with overrepresented
104 species. To elucidate the types of interactions (bacterial competition or facilitation), we
105 selectively removed species from the inoculum (one at a time). Our high-throughput system
106 and the modular approach using defined species and habitats is well suited for disentangling
107 abiotic factors and identifying interspecies interactions, the two key components for
108 scrutinizing mechanisms of bacterial community assembly.
109

110 ## Results

111 *Convergence of bacterial community composition in structured habitats*

112 We manipulated the initial composition of the synthetic bacterial community inoculum
113 (Supplementary Table S2) by targeted overrepresentation and omission of selected members
114 and followed the development of community composition growing in an unstructured batch
115 habitat and structured microcosms kept under 'wet' and 'dry' conditions (Fig. 1). The absolute
116 abundance for each community member, estimated by the number of species 'genome
117 equivalents' (≈number of bacterial cells, see *Materials and Methods*) in each microcosm shows
118 an increase of the total community under all conditions from inoculation to 2 days and further
119 at 6 days of incubation (Fig. 2). The resulting species abundance varied by several orders of
120 magnitude from virtually undetected to 8×10^8 cells per microcosm (representing 3.2×10^9 cells
121 per g glass beads) for the most abundant species (Fig. 3). Community composition in all
122 microcosms were dominated by gammaproteobacteria (*Pseudomonas protegens*, *Pseudomonas*
123 *stutzeri*, *Escherichia coli*), irrespective of time or initial species ratio (Fig. 3). Remarkably, the
124 absolute and relative abundance of these three dominant species was consistent across replicates

and determined primarily by the presence or absence of microcosm spatial structure and by the hydration status of structured habitats. While *P. protegens* and *E. coli* dominated liquid batch microcosms, *P. stutzeri* was the most abundant species in microcosms containing glass beads, with this trend increasing over time (Fig. 3). The marked changes in relative abundance of dominant species between structured and non-structured microcosms seem to be controlled by the growth of *P. stutzeri*, whose abundance was poor in batch (10^4-10^5) but highest of all species in glass bead microcosms both under wet or dry conditions ($\approx 10^8$, an increase of 3-4 orders of magnitude). Spearman's rank correlations between the Bray-Curtis similarities of microbial community composition in all samples confirmed *P. stutzeri* as main driver for the observed patterns (73 %). Importantly, the divergence of community compositional patterns observed in structured and non-structured microcosms was not driven by the total size of the bacterial community, which was highest in wet structured habitats (up to 10^9 cells per microcosm) and similarly lower in liquid and dry structured habitats (Figs. 2A and 3). Principal coordinate analysis (PCoA) of Bray-Curtis dissimilarities (Fig. 2B) shows a distinct cluster of bacterial communities from liquid habitats separated from communities in structured microcosms. The structured habitats communities were grouped based on hydration condition ('wet' and a 'dry' clusters). Additionally, the different sampling times (2 days and 6 days) formed delimited sub-clusters within their respective hydration conditions (Fig. 2 B). High similarity of community structure within the same habitat at 2 and 6 days are further confirmed by ANOSIM pairwise comparison of each habitat and time point (Fig. 2 C). Moreover, ANOSIM statistics also underscore strong differences in community structure between batch culture incubation and communities from structured microcosm habitats.

Manipulation of initial species ratio has limited effects on community convergence

The overrepresentation of individual species in the initial inoculum (Fig. 1) did not affect the overall dominance of gammaproteobacteria in unstructured and structured habitats (Fig. 3A).

While overrepresentation resulted in significant changes in community composition, those changes were transient and waned or disappeared after 6 days of incubation (most notably in the case of *P. stutzeri*, *P. protegens*, *E. coli* and *Burkholderia xenovorans*). After 6 days, the relative abundance patterns of the dominant species were virtually unaffected by a 100-fold increase in initial abundance of each species compared to the others, with the exception of *P. protegens* that persisted at high abundance at 2 and 6 days when overrepresented in structured habitats (Fig. 3A). Similarly, in most cases the patterns of dominant species persisted despite omission of selected species in the initial inoculum. Nevertheless, marked changes occurred when one of the members of the dominant trio of gammaproteobacteria was removed (Fig. 3B). Specifically, the removal of *P. stutzeri* in structured habitats led to increased *P. protegens* growth and relative abundance, which produced a pattern similar to that of liquid habitats. *Arthrobacter chlorophenolius* was also stimulated by the removal of *P. stutzeri*, but only in dry structured habitats, and the effect was no longer visible after 6 days. *P. protegens*, once removed from liquid habitats, was replaced by a diversity of other species (*P. stutzeri*, *E. coli, A. chlorophenolicus, B. xenovorans, Bacillus subtilis*) with high reproducibility among replicate microcosms (Fig. 3B).

Signatures of initial species overrepresentation persists in structured habitats

We systematically tested the consequences of a 100-fold increase of one species over the others, one species at a time, in the mix inoculum. Although the relative abundance patterns of dominant species persisted, as discussed above, imprints of this initial manipulation of community composition were detected in the absolute abundance counts. These compositional signatures were prominent in structured habitats (wet and dry), exhibiting a 'staircase' pattern of absolute abundance heatmap (Fig. 3A). Two days after inoculation, this imprint was visible for all 11 species in the community in structured habitats, whereas in liquid habitats its persistence was limited to five species (*P. stutzeri, A. chlorophenolicus, B. xenovorans, B.*

177 *subtilis* and *Xanthobacter autotrophicus,* Fig. 3A). Moreover, this characteristic pattern was
178 confirmed by the analysis of significant effects of one species initial overrepresentation over
179 the same species final abundance (Fig. 4A and Supplementary Fig. S2) with significant increase
180 for all 11 overrepresented community members ($p < 0.05$) in structured wet habitats (Fig. S2).
181
182 *Species overrepresentation or removal from inoculum uncovers interspecific interactions*
183 We further analyzed the absolute counts data to identify causal relationships between the
184 overrepresentation or omission of a given species and the absolute increase or decrease of
185 another bacterial species abundance (measured as number of genome equivalents), which we
186 define here respectively as positive and negative effects. We compared species abundances in
187 microcosms inoculated with uneven initial species mixtures with abundances in microcosms
188 inoculated with an even mix of species serving as a control (Fig. 1B), for each treatment and
189 time point. Selected results presented in Fig. 4 (and full results in Supplementary Fig. S2) show
190 the detected changes in the abundance of one species with respect to the control (with a >5-fold
191 change threshold contingent to a p-value<0.05). The total number of detected positive and
192 negative effects in liquid habitats was higher than in structured habitats in both cases of species
193 overrepresentation and omission (Fig. 4 and Supplementary Fig. S2). While the number of
194 detected positive effects increased with time in liquid habitats, it decreased in structured habitats
195 (Fig. 4). Negative effects (i.e., decrease in another species' abundance) were observed for one
196 single case in liquid habitats at day 2 (decrease of *B. subtilis* in response to overrepresentation
197 of *P. protegens*), but were frequent in structured habitats, especially after 6 days (Fig. 4 and
198 Supplementary Fig. S2). Results obtained from species omission suggested more and stronger
199 competitive interactions in liquid than in structured habitats (Fig. 4B and Supplementary Fig.
200 S2). After 6 days in liquid, the removal of *P. protegens* had permitted significant growth
201 increase in five other species: *A. chlorophenolicus*, *B. subtilis*, *B. xenovorans*, *E. coli* and *P.*
202 *stutzeri*, but this was not the case in structured habitats (Fig. 4B and Supplementary Fig. S2).

We identified a number of reciprocal responses to overrepresentation and omission, that is, instances where a species both increased in absence and decreased in overrepresentation of another species (or vice versa): *E. coli* in response to *S. violaceoruber* and *X. autotrophicus* (wet structured); *A. chlorophenolicus* in response to *P. stutzeri* (dry structured); *B. subtilis* in response to *P. protegens* (liquid).

Discussion

The study highlights dynamic adjustments in species composition of a well-defined bacterial community (Fig. 1) grown in different habitats with two distinctly different outcomes: (1) a community dominated by *P. protegens* for liquid habitat; or (2) a community dominated by *P. stutzeri* in porous and structured habitat (Fig. 3). Under all conditions gammaproteobacteria dominated the microcosms, which suggested a faster or more efficient use of the nutrients available in the growth medium. However, the difference between (1) and (2) could not be attributed to nutrient resources (invariant across microcosms), nor to the total growth of the community (Fig. 2A). We propose that, to account for this discrepancy, the nature of the habitat is the primary determining factor (i.e., the presence or absence of physical structure with microscopic spatial arrangement of habitats) (Fig. 3A). Generally, the results supported the hypothesis that spatially structured habitats exert strong influence on growth, interactions and assembly of bacterial communities. Additionally, the nature of the habitat and interactions is not only determined by the solid phase (glass beads), but by the hydration state (aqueous phase) as well. The organization of the aqueous phase near water saturation (‘wet’) or under relatively drier conditions (‘dry’) had a significant influence on species abundance. With ‘wet’ porous habitats giving rise to bacterial community composition similar to liquid habitats, with higher abundances of *P. protegens* and *E. coli* and lower abundance of *A. chlorophenolicus* (Fig. 2A). This result emphasizes the importance of aqueous phase organization on habitat connectivity

and community composition, as also supported by previous experimental and modelling studies (Borer et al 2019, Kim and Or 2017, Kleyer et al 2019).

The use of a synthetic bacterial community enabled systematic manipulation of initial species composition in microcosms (i.e., with 100-fold relative increase or removal of individual species, Fig. 1). Our results showed that irrespective of initial bacterial species ratio, the community composition drifted from an initially even abundance to similar patterns dominated by *Pseudomonas* species. Even after 6 days, the initial differences in species ratio did not alter the relative abundance patterns with respect to the most abundant species in the community (except when the dominant species *P. protegens* or *P. stutzeri* were omitted from the inoculum) (Fig. 2). Remarkably, the imprint of initially overrepresented bacterial species was preserved in communities grown in porous media with structured habitats (Fig. 2A, Fig. 4A, and Supplementary Fig. S2). This suggests that physical structure and aqueous habitats forming between glass beads may either stimulate species growth or reduce interspecific interactions irrespective details of the hydration status. This translates to a stabilizing effect of structured environments that preserves initial community composition for extended periods relative to community composition in liquid culture with potential implications for engineering stable microbial communities (Ben Said et al 2020, Lindemann et al 2016).

In addition to bacterial-habitat interactions, we seek insights on interspecific interactions that shape community composition and the roles of community members and their collective functioning. Selective initial overrepresentation or omission triggered significant changes in different species' final abundances (Figs. 2 and 4). In a background of similar resource availability, we link these changes to the onset of competitive or facilitative interactions between various species during growth (Bruno et al 2003, Ghoul and Mitri 2016). Competition is expected to dominate interactions in our system, because all species grow independently to high cell densities in the complex liquid medium (a nutritious mix of protein digests with glucose and mannitol as additional carbon sources) (Kleyer et al 2019). This is

supported by the drift from an initially even community composition to a highly uneven composition observed in all treatments after 2 days, with gammaproteobacteria out-competing other phyla (Fig. 2). It is further supported by the omission of one of those dominant species resulting in higher abundances of similar competitors, notably the replacement of *P. protegens* by *P. stutzeri* and vice versa (the two *Pseudomonas* species are closely related phylogenetically and share certain traits such as fast growth on rich media) (Fig. 4B). In addition to competing for nutrients and space, the bacterial species in the community might also directly antagonize each other (Little et al 2008). *P. protegens*, in particular, is known to secrete a variety of antimicrobial metabolites (Ramette et al 2011) and possesses a Type VI secretion system that is involved in contact-dependent elimination of competitors (Vacheron et al 2019). Such antagonizing mechanisms could potentially also explain the marked effects of *P. protegens* omission in liquid cultures (Fig. 4B). By contrast, facilitation (e.g., metabolic cross-feeding between species) is less expected considering that the growth medium is complex (thus obscuring trophic dependencies (D'Souza et al 2018)) and non-toxic (Piccardi et al 2019). Overall, our results from species omission experiments supported these expectations on the nature of interactions in our system (Fig. 4B, Supplementary Fig. S2). The use of a synthetic ecology approach was here decisive to clearly disentangle species interactions from habitat filtering (Ghoul and Mitri 2016, Vorholt et al. 2017); the impossibility to do so remains an inherent limitation in network analyses of microbial communities from natural habitats (Röttjers and Faust 2018).

The number of detected changes suggesting species interactions was overall higher and largely positive in liquid compared to structured habitats (Fig. 4 and Supplementary Fig. S2). We found that in response to species overrepresentation in liquid habitats, other phylogenetically distant members exhibited an increase in abundance (e.g., increase of *B. subtilis* or *B. xenovorans* facilitated growth of five community members from four different phyla), which could indicate potential cross-feeding due to metabolic dissimilarities. Somewhat

surprising are results from species omission that suggest prevalence of facilitative interactions in structured habitats, while results from species overrepresentation suggested the converse (Fig. 4 and Supplementary Fig. S2). However, we note that overrepresenting and omitting species are not strictly symmetrical manipulations, and in that context we consider species omission to be a more definitive arbiter in determining species interactions (see also for example Gutiérrez and Garrido, 2019).

Importantly, our results demonstrate that porous and structured microhabitats modulate the number, type and strength of interspecies interactions. These effects have been previously suggested for small bacterial assemblages of 2-3 species (Borer et al 2018, Kim et al 2008). As noted above, most natural habitats harbour complex spatial structures that likely mitigate competitive effects. This understanding challenges a widespread (albeit debated) view that competition dominates interactions among microorganisms in nature (Foster and Bell 2012). We surmise that the experimental reliance on liquid cultures to study microbial interaction processes may overemphasize the prevalence of interspecies competition within microbial communities in nature (Foster and Bell 2012, Rivett et al 2016).

The role of spatial structures highlights certain limitations of the widespread use well-mixed liquid media to study bacterial interactions and community assembly. The simplicity and reproducibility offered by such media comes with a bias of the behaviour of such communities in natural and structured environments (i.e., soil or human gut). These differences are rooted in the complex spatial arrangement of solids, liquid and gas phases at the microscale and their impacts on the diffusion, motility and interspecific interactions in most natural environments (Tecon and Or 2017, Vos et al 2013). Consequently, we argue that the physical spatial structures of microbial habitats is a central element necessary for any accurate prediction of bacterial community dynamics and stability, alongside well recognized factors such as the type and diversity of carbon sources (Goldford et al 2018, Zegeye et al 2019).

Arguably, a fundamental goal of microbial ecology is to uncover the ecological mechanisms that permit the coexistence of many diverse species within a shared environment (Tilman 1982). Among the identified mechanisms, niche partitioning is often predicted to play a major role (Saleem et al 2015). Niche partitioning can refer to differential use of resources ('ecological' or 'metabolic' niche) (Saleem et al 2015) and to segregation in distinct spatial areas ('spatial' niche) (Ghoul and Mitri 2016). We conclude from our results that the latter is more likely to be at play in structured microcosms (containing glass beads at various hydration states), hence supporting species coexistence. In general, when considering that many natural habitats are porous media (notably, soil) characterized by physico-chemical gradients and spatial structures, we may contemplate a vast diversity of spatial niches arising that are absent in liquid environments (Bickel and Or 2020, Raynaud and Nunan 2014, Tecon and Or 2017). As noted above, spatial structuring leads to another complementary mechanism promoting bacterial species coexistence: the abatement of strong ecological interactions (positive or negative) between species that perturb the community. This mechanism was notably proposed to account in part for the observed stability of the human gut microbiome (Coyte et al 2015).

Results presented here underscore the crucial role of habitat structure, key for our understanding of processes in natural bacterial communities inhabiting heterogeneous environments where structures define and stabilize composition and dynamics that essentially impact community functioning (e.g. gut- and soil microbiota). Lasting effects from directed manipulation of bacterial community composition are fundamental for communities used as probiotics, in food production or for environmental restoration, remediation and in biocontrol. Linking effects of hydration and the physical spatial structure with dynamics in a defined bacterial community offers a useful tool in sustainable engineering of community composition.

Materials and Methods

Bacterial strains, culture conditions and synthetic community assembly

We assembled a synthetic bacterial community comprised of 11 species listed in Fig. 1. Bacterial strains were obtained from the Leibniz-Institute German collection of microorganisms (DSMZ): A6 (DSM12829), 168 (DSM402), LB400 (DSM17367), MG1655 (DSM18039), DSM20030, T27 (DSM17841), CHA0 (DSM19095), CMT.9.A (DSM4166), CFN 42 (DSM11541), A3(2) (DSM40783), 7C (DSM432). All bacterial strains were cultured on 0.1x tryptic soy broth (TSB) agar plates (VWR International, Leuven, Belgium) supplemented with 1% mannitol (TSBM) at 25 °C (mannitol sustains the growth of *R. etli*). For inoculation, 48h-old plates were scraped with a sterile spartel and bacteria were suspended in PBS (Phosphate Buffered Saline) solution with pH 7.4 (Gibco, life technologies Europe, Bleiswijk, Netherlands). Bacterial biomass was measured using optical density at 600 nm (OD_{600}). *Rhizobium etli* and *Xanthobacter autotrophicus* secreted copious amount of extracellular polymeric substances (slime) when grown on agar plate, and for that reason these two species were subjected to an additional washing step in PBS in order to remove slime prior to OD_{600} measurement. *Streptomyces violaceoruber* grows as a mycelium, which can bias OD_{600} measurement. Therefore, *S. violaceoruber* was further treated in an ultrasonic bath (Branson Ultrasonics, Danbury, Connecticut, United States) at 40 kHz for 30 seconds in PBS to homogenize the bacterial suspension prior to OD_{600} measurement. All bacterial communities were prepared with the same final size of approx. 5.5x 10^4 cells (calculated from OD_{600} measurement) with PBS used for dilutions. For the community containing all 11 members, individual species with an OD_{600} of 0.1 were combined in equal proportions and further diluted with PBS to approx. 5 000 cells of each member resulting in a total community size of ~5.5x 10^4 cells. For the overrepresentation one member was added with 100x fold higher initial abundance (~50 000 cells) to the other ten species with ~500 cells each (total community size

354 5.5x 10^4 cells). Inocula missing one species were prepared by combining 10 out of 11 members
355 at approx. 5'500 cells each, resulting in communities of ten members with a total community
356 size of ~5.5x 10^4 cells. As culture medium, 240 µl of 0.1x TSBM were added to each
357 microhabitat and microcosms were inoculated with 10 µl of the bacterial community. The same
358 procedure was applied to inoculate liquid cultures in 96-well system kept in parallel to the
359 experimental set-up at constant temperature of 25 °C.
360
361 *Bacterial community growth in microcosms*
362 For details on microcosms preparation and incubation, see Supplementary Methods. Briefly,
363 structured microcosms were set-up in multi-well plates with a 0.22 µm filter membrane at the
364 bottom of the well (Merck, Darmstadt, Germany) and containing 250 mg of sterile glass beads
365 (with diameter of 80 to 120 µm) per well. Microcosms were connected via a saturated porous
366 plate to a sterile medium reservoir containing 800 ml of saline solution. The height of the liquid
367 column (the difference in elevation between the microcosms surface and the liquid medium
368 level in the reservoir) prescribed the liquid tension and thus the hydration conditions in the
369 porous plate and the glass-beads microcosms. In parallel, conventional multiwell plates were
370 used for homogeneous liquid microcosms. Each multiwell plate contained 80 parallel
371 microcosms with 20 different initial inocula. An inoculum with the 11 species at equal
372 proportions; 11 with one member 100x overrepresented and 8 with one member missing with
373 four replicate wells per community inoculum. Two liquid habitat multiwell plates and four
374 structured habitat multiwell plates (2 WET and 2 DRY, Fig. 1) were prepared. One plate of
375 each treatment was sacrificed after 2 and 6 days of incubation at 25 °C for total DNA extraction
376 from microcosms.
377
378 *DNA extraction and quantification*

379 The microcosms contents were transferred by pipetting to individual 1.2 ml tubes (Brand GmbH
380 + co KG, Wertheim, Germany), immediately frozen in liquid nitrogen and stored at -80 °C. At
381 the end of the experiment all samples were thawed on ice, and DNA was extracted using the
382 DNeasy blood and tissue kit (Qiagen, Hilden, Germany) following the manufacturer's
383 instructions for increased cell lysis efficiency. DNA concentration was quantified
384 fluorometrically using the Qubit dsDNA HS assay kit (Thermo Fischer Scientific). See
385 Supplementary Methods for details.
386
387 *Microfluidic quantitative real-time PCR*
388 Microfluidic quantitative PCR was performed using a Fluidigm 192x24 Dynamic Array
389 (Fluidigm Corporation, San Francisco, CA, USA). Details on the qPCR method using assay
390 chips with integrated fluidic circuits (IFCs) for high throughput is described in previous work
391 (Kleyer et al 2017, Kleyer et al 2019), including a nested-PCR approach where the 16S rRNA
392 gene is preamplified with universal primers to enhance the signal for real-time PCR
393 quantification of individual community members via species-specific PCR primers
394 (Supplementary Table S1). For more details, see Supplementary Methods.
395
396 *Data Analysis and Statistics*
397 Real-time quantitative PCR data were analysed with the software provided by the manufacturer
398 (Fluidigm Corporation). We used standard curves obtained from a mixture of pure genomic
399 DNA from each species to quantify the absolute abundance of individual species in the
400 microcosms (Supplementary Fig. S1). This absolute abundance was estimated for a given
401 species as the number of 'genome equivalents' per unit mass genomic DNA based on
402 information on each species genome size (for more details see reference (Kleyer et al 2019)).
403 Total species abundance in each microcosm was back-calculated from total community DNA
404 extracted per microcosm (Qubit high-sensitivity assay for dsDNA; Thermo Fisher Scientific)

405 (Fig. 2A). Measurement values <1 genome in DNA template were not reported. A Bray-Curtis
406 dissimilarity matrix was calculated in R (www.r-project.org) with the R package vegan. To
407 show most of the variation we performed a principle coordinate analysis PCoA (R-package
408 vegan) and visualized the result with ggplot2 (Fig. 2B). Analysis of similarity (ANOSIM) was
409 performed with the R-package vegan to obtain statistical R-values for dissimilarity between
410 time points and treatments (Fig. 2C). Interspecific interactions reflected in positive and negative
411 effects of overrepresented- or omitted community members were calculated from absolute
412 abundance data by comparing the abundance of each species per sample to the abundance of
413 the same species in the control microcosms (inoculated with an even mix of all species).
414 Variations (increase or decrease) in absolute abundances were deemed significant and thus
415 represented when >5-fold with a p-value <0.05 (using a two-tailed t-test on 4 replicates).
416

Acknowledgments

We thank Aria Minder and Silvia Kobel from the Genetic Diversity Center of ETH Zurich for help with the Fluidigm high throughput qPCR. Financial support for this work came from the Swiss National Science Foundation (project number 31003A_182734). We declare that the research was conducted in the absence of any commercial or financial relationships that could be construed as a potential conflict of interest.

Author Contributions

H.K., R.T. and D.O. designed the research. H.K. performed the experimental research and analyzed data. H.K., R.T. and D.O. wrote the manuscript.

References

Abreu CI, Friedman J, Andersen Woltz VL, Gore J (2019). Mortality causes universal changes in microbial community composition. *Nature Communications* **10:** 2120.

Afshinnekoo E, Meydan C, Chowdhury S, Jaroudi D, Boyer C, Bernstein N *et al* (2015). Geospatial Resolution of Human and Bacterial Diversity with City-Scale Metagenomics. *Cell Systems* **1:** 72-87.

Bahram M, Hildebrand F, Forslund SK, Anderson JL, Soudzilovskaia NA, Bodegom PM *et al* (2018). Structure and function of the global topsoil microbiome. *Nature* **560:** 233-237.

Bai Y, Müller DB, Srinivas G, Garrido-Oter R, Potthoff E, Rott M *et al* (2015). Functional overlap of the Arabidopsis leaf and root microbiota. *Nature* **528:** 364.

Ben Said S, Tecon R, Borer B, Or D (2020). The engineering of spatially linked microbial consortia – potential and perspectives. *Curr Opin Biotechnol* **62:** 137-145.

Bickel S, Or D (2020). Soil bacterial diversity mediated by microscale aqueous-phase processes across biomes. *Nature Communications* **11:** 116.

Borer B, Tecon R, Or D (2018). Spatial organization of bacterial populations in response to oxygen and carbon counter-gradients in pore networks. *Nature communications* **9:** 769.

Borer B, Ataman M, Hatzimanikatis V, Or D (2019). Modeling metabolic networks of individual bacterial agents in heterogeneous and dynamic soil habitats (IndiMeSH). *PLoS Comp Biol* **15:** e1007127.

Brennan, F. P., O'Flaherty, V., Kramers, G., Grant, J., & Richards, K. G. (2010). Long-term persistence and leaching of Escherichia coli in temperate maritime soils. Applied and environmental microbiology, 76(5), 1449-1455.

Brenner, D. J., Krieg, N. R., Staley, J. T., & Garrity, G. (2005). Bergey's manual of systematic bacteriology, Vol 2: The Proteobacteria. NY: Springer.

Bruno JF, Stachowicz JJ, Bertness MD (2003). Inclusion of facilitation into ecological theory. *Trends Ecol Evol* **18:** 119-125.

Cairns J, Jokela R, Hultman J, Tamminen M, Virta M, Hiltunen T (2018). Construction and characterization of synthetic bacterial community for experimental ecology and evolution. *Frontiers in genetics* **9:** 312.

Carlström CI, Field CM, Bortfeld-Miller M, Müller B, Sunagawa S, Vorholt JA (2019). Synthetic microbiota reveal priority effects and keystone strains in the Arabidopsis phyllosphere. *Nature Ecology & Evolution* **3:** 1445-1454.

Chodkowski JL, Shade A (2017). A Synthetic Community System for Probing Microbial Interactions Driven by Exometabolites. *mSystems* **2:** e00129-00117.

476 Costea PI, Hildebrand F, Arumugam M, Bäckhed F, Blaser MJ, Bushman FD *et al* (2018).
477 Enterotypes in the landscape of gut microbial community composition. *Nature Microbiology*
478 **3:** 8-16.
479
480 Coyte KZ, Schluter J, Foster KR (2015). The ecology of the microbiome: Networks,
481 competition, and stability. *Science* **350:** 663-666.
482
483 D'Souza G, Shitut S, Preussger D, Yousif G, Waschina S, Kost C (2018). Ecology and evolution
484 of metabolic cross-feeding interactions in bacteria. *Natural Product Reports* **35:** 455-488.
485
486 Delgado-Baquerizo M, Oliverio AM, Brewer TE, Benavent-González A, Eldridge DJ, Bardgett
487 RD *et al* (2018). A global atlas of the dominant bacteria found in soil. *Science* **359:** 320-325.
488
489 Ebrahimi A, Or D (2015). Hydration and diffusion processes shape microbial community
490 organization and function in model soil aggregates. *Water Resour Res***:** n/a-n/a.
491
492 Enke TN, Datta MS, Schwartzman J, Cermak N, Schmitz D, Barrere J *et al* (2019). Modular
493 Assembly of Polysaccharide-Degrading Marine Microbial Communities. *Curr Biol* **29:** 1528-
494 1535.e1526.
495
496 Foster Kevin R, Bell T (2012). Competition, Not Cooperation, Dominates Interactions among
497 Culturable Microbial Species. *Curr Biol* **22:** 1845-1850.
498
499 Friedman J, Higgins LM, Gore J (2017). Community structure follows simple assembly rules
500 in microbial microcosms. *Nature Ecology &Amp; Evolution* **1:** 0109.
501
502 Fu, He, et al. "Ecological drivers of bacterial community assembly in synthetic phycospheres."
503 Proceedings of the National Academy of Sciences 117.7 (2020): 3656-3662.
504
505 Ghoul, Melanie, and Sara Mitri. "The ecology and evolution of microbial competition." Trends
506 in microbiology 24.10 (2016): 833-845.
507
508 Gokhale S, Conwill A, Ranjan T, Gore J (2018). Migration alters oscillatory dynamics and
509 promotes survival in connected bacterial populations. *Nature Communications* **9:** 5273.
510
511 Goldford JE, Lu N, Bajić D, Estrela S, Tikhonov M, Sanchez-Gorostiaga A *et al* (2018).
512 Emergent simplicity in microbial community assembly. *Science* **361:** 469-474.
513
514 Ibarbalz FM, Henry N, Brandão MC, Martini S, Busseni G, Byrne H *et al* (2019). Global Trends
515 in Marine Plankton Diversity across Kingdoms of Life. *Cell* **179:** 1084-1097.e1021.
516
517 Kehe J, Kulesa A, Ortiz A, Ackerman CM, Thakku SG, Sellers D *et al* (2019). Massively
518 parallel screening of synthetic microbial communities. *Proceedings of the National Academy*
519 *of Sciences* **116:** 12804-12809.
520
521 Kim HJ, Boedicker JQ, Choi JW, Ismagilov RF (2008). Defined spatial structure stabilizes a
522 synthetic multispecies bacterial community. *Proceedings of the National Academy of Sciences*
523 **105:** 18188-18193.
524
525 Kim M, Or D (2017). Hydration status and diurnal trophic interactions shape microbial
526 community function in desert biocrusts. *Biogeosciences* **14:** 5403-5424.

Kleyer H, Tecon R, Or D (2017). Resolving Species Level Changes in a Representative Soil Bacterial Community Using Microfluidic Quantitative PCR. *Frontiers in Microbiology* **8**.

Kleyer H, Tecon R, Or D (2019). Rapid shifts in bacterial community assembly under static and dynamic hydration conditions in porous media. *Appl Environ Microbiol***:** AEM.02057-02019.

Lawson CE, Harcombe WR, Hatzenpichler R, Lindemann SR, Löffler FE, O'Malley MA *et al* (2019). Common principles and best practices for engineering microbiomes. *Nature Reviews Microbiology* **17:** 725-741.

Liang, Y., Meggo, R., Hu, D., Schnoor, J. L., & Mattes, T. E. (2014). Enhanced polychlorinated biphenyl removal in a switchgrass rhizosphere by bioaugmentation with Burkholderia xenovorans LB400. Ecological engineering, 71, 215-222.

Lindemann SR, Bernstein HC, Song H-S, Fredrickson JK, Fields MW, Shou W *et al* (2016). Engineering microbial consortia for controllable outputs. *ISME J*.

Little AEF, Robinson CJ, Peterson SB, Raffa KF, Handelsman J (2008). Rules of Engagement: Interspecies Interactions that Regulate Microbial Communities. *Annu Rev Microbiol* **62:** 375-401.

Lowery NV, Ursell T (2019). Structured environments fundamentally alter dynamics and stability of ecological communities. *Proceedings of the National Academy of Sciences* **116:** 379-388.

Meroz, N., Tovi, N., Sorokin, Y. et al. Community composition of microbial microcosms follows simple assembly rules at evolutionary timescales. Nat Commun 12, 2891 (2021). https://doi.org/10.1038/s41467-021-23247-0

Nadell CD, Drescher K, Foster KR (2016). Spatial structure, cooperation and competition in biofilms. *Nat Rev Micro* **14:** 589-600.

Piccardi P, Vessman B, Mitri S (2019). Toxicity drives facilitation between 4 bacterial species. *Proceedings of the National Academy of Sciences* **116:** 15979-15984.

Ramette A, Frapolli M, Saux MF-L, Gruffaz C, Meyer J-M, Défago G *et al* (2011). Pseudomonas protegens sp. nov., widespread plant-protecting bacteria producing the biocontrol compounds 2,4-diacetylphloroglucinol and pyoluteorin. *Syst Appl Microbiol* **34:** 180-188.

Raynaud X, Nunan N (2014). Spatial Ecology of Bacteria at the Microscale in Soil. *PLoS ONE* **9:** e87217.

Rivett DW, Scheuerl T, Culbert CT, Mombrikotb SB, Johnstone E, Barraclough TG *et al* (2016). Resource-dependent attenuation of species interactions during bacterial succession. *The ISME Journal* **10:** 2259-2268.

Röttjers L, Faust K (2018). From hairballs to hypotheses–biological insights from microbial networks. *FEMS Microbiol Rev* **42:** 761-780.

Saleem M, Pervaiz ZH, Traw MB (2015). Theories, Mechanisms and Patterns of Microbiome Species Coexistence in an Era of Climate Change. *Microbiome Community Ecology: Fundamentals and Applications*. Springer International Publishing: Cham. pp 13-53.

Singh, P., & Tiwary, B. N. (2017). Optimization of conditions for polycyclic aromatic hydrocarbons (PAHs) degradation by Pseudomonas stutzeri P2 isolated from Chirimiri coal mines. Biocatalysis and agricultural biotechnology, 10, 20-29.

Tecon R, Or D (2017). Biophysical processes supporting the diversity of microbial life in soil. *FEMS Microbiol Rev* **41:** 599-623.

Tecon R, Ebrahimi A, Kleyer H, Levi SE, Or D (2018). Cell-to-cell bacterial interactions promoted by drier conditions on soil surfaces. *Proceedings of the National Academy of Sciences* **115:** 9791-9796.

Tilman D (1982). *Resource competition and community structure*. Princeton university press.

Tilman D (1994). Competition and biodiversity in spatially structured habitats. *Ecology* **75:** 2-16.

Vacheron J, Péchy-Tarr M, Brochet S, Heiman CM, Stojiljkovic M, Maurhofer M *et al* (2019). T6SS contributes to gut microbiome invasion and killing of an herbivorous pest insect by plant-beneficial Pseudomonas protegens. *The ISME Journal* **13:** 1318-1329.

Voges MJ, Bai Y, Schulze-Lefert P, Sattely ES (2019). Plant-derived coumarins shape the composition of an Arabidopsis synthetic root microbiome. *Proceedings of the National Academy of Sciences* **116:** 12558-12565.

Vorholt JA, Vogel C, Carlström CI, Müller DB (2017). Establishing causality: opportunities of synthetic communities for plant microbiome research. *Cell host & microbe* **22:** 142-155.

Vos M, Wolf AB, Jennings SJ, Kowalchuk GA (2013). Micro-scale determinants of bacterial diversity in soil. *FEMS Microbiol Rev***:** n/a-n/a.

Wang G, Or D (2013). Hydration dynamics promote bacterial coexistence on rough surfaces. *ISME J* **7:** 395-404.

Westerberg, K., Elväng, A. M., Stackebrandt, E., & Jansson, J. K. (2000). Arthrobacter chlorophenolicus sp. nov., a new species capable of degrading high concentrations of 4-chlorophenol. *International Journal of Systematic and Evolutionary Microbiology*, *50*(6), 2083-2092.

Widder S, Allen RJ, Pfeiffer T, Curtis TP, Wiuf C, Sloan WT *et al* (2016). Challenges in microbial ecology: building predictive understanding of community function and dynamics. *The ISME journal*.

Zegeye EK, Brislawn CJ, Farris Y, Fansler SJ, Hofmockel KS, Jansson JK *et al* (2019). Selection, Succession, and Stabilization of Soil Microbial Consortia. *MSystems* **4:** e00055-00019.

Figures

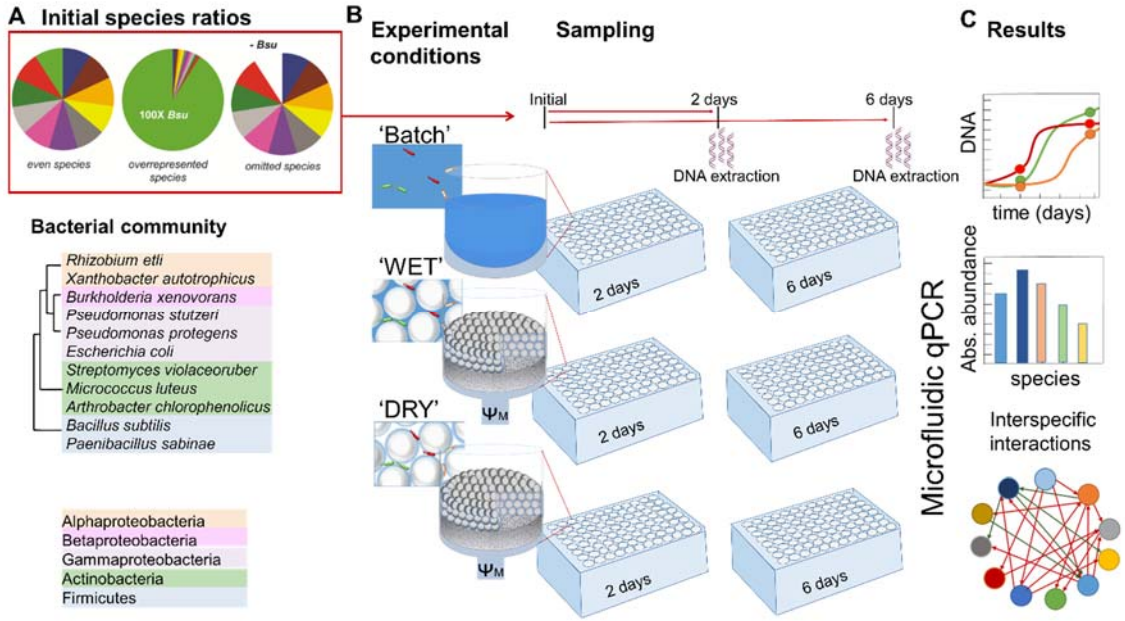

Figure 1. Synthetic ecology as experimental approach. (A) Synthetic bacterial community of 11 phylogenetically diverse species. We manipulated the initial species ratio in the community as follows. Species were mixed in even proportions, in uneven proportions with one species being a 100-fold overrepresented, and in even proportions but with one species removed. An example with *B. subtilis* is shown. (B) Microcosms were set up in multi-well plates containing only liquid medium ('batch'), or liquid medium and glass beads (diameter ≈100 µm) to provide a spatial structure to the habitat, with prescribed hydration status in the microcosms permitting us to maintain relatively 'wet' or 'dry' conditions in the structured habitats. Even and uneven species mixes were used as inocula. Two multi-well plates per treatment were prepared, and sacrificed after 2 and 6 days of incubation. Beads and bacteria are shown for illustration purposes and their relative size is not on scale. (C) Microfluidic-based qPCR was used to resolve bacterial community composition at the species level to obtain relative and absolute abundance data.

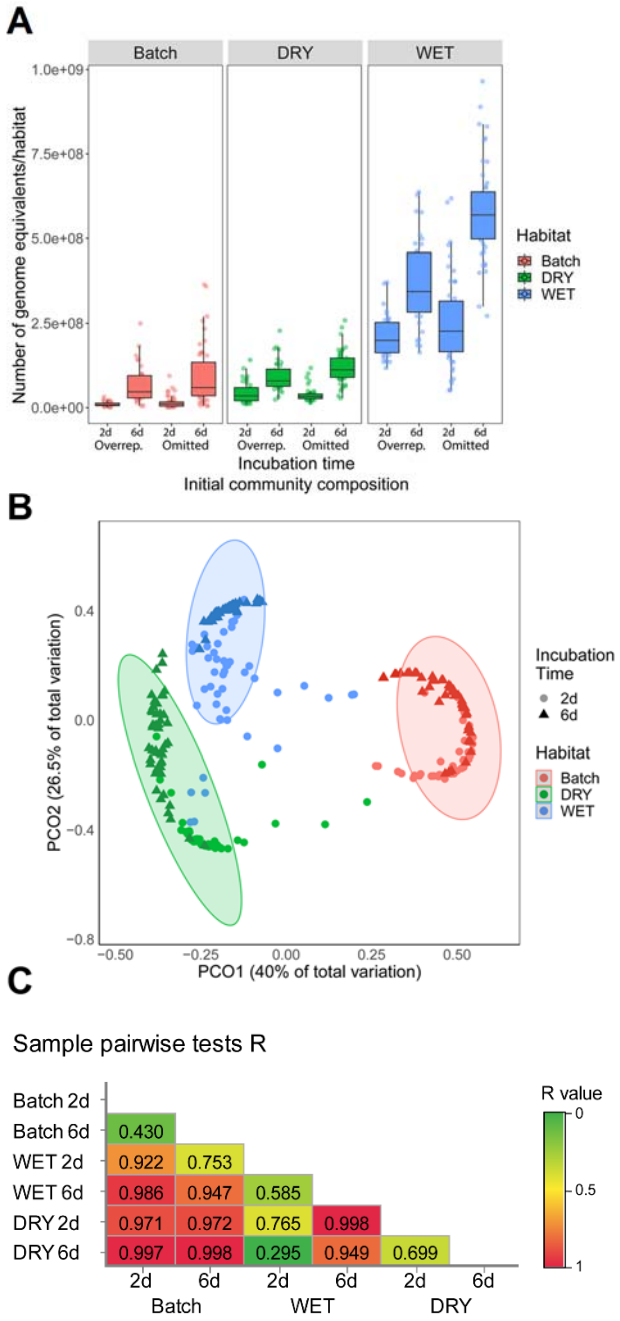

Figure 2. (A) Total bacterial community size as function of treatment and time. Boxplots show the estimated sum of all species in the community, expressed as number of genome equivalents per microcosm. Total abundances were systematically higher in wet structured microcosms compared to dry structured and batch microcosms, and after 6 days compared to 2 days. Omitting or 100x overrepresentation (Overrep.) of a species did not appear to affect the total counts. (B) PCoA plot based on Bray-Curtis dissimilarity calculated for microcosms inoculated with an even mix of species or mixes of species containing an overrepresented member.

654 Clustering indicates the largest separation between communities incubated in unstructured
655 batch microcosms and in glass-bead structured microcosms under WET and DRY conditions,
656 ellipses enclose 95% of the data points for each condition. Further separation is observed for
657 the time of sampling (2 days and 6 days) forming partially overlapping sub-clusters. (C)
658 Pairwise comparisons of dissimilarity between treatments were calculated with ANOSIM. R
659 values close to 1.0 (red) suggest high dissimilarity between treatment groups. Communities in
660 batch habitats strongly differ from communities growing in structured microcosms under DRY
661 and WET conditions. Moreover, differences in community structure were observed between
662 communities from structured microcosms kept under DRY and WET conditions. Community
663 structure within the same treatment at the early and late time point show intermediate R values
664 indicating some overlap.
665

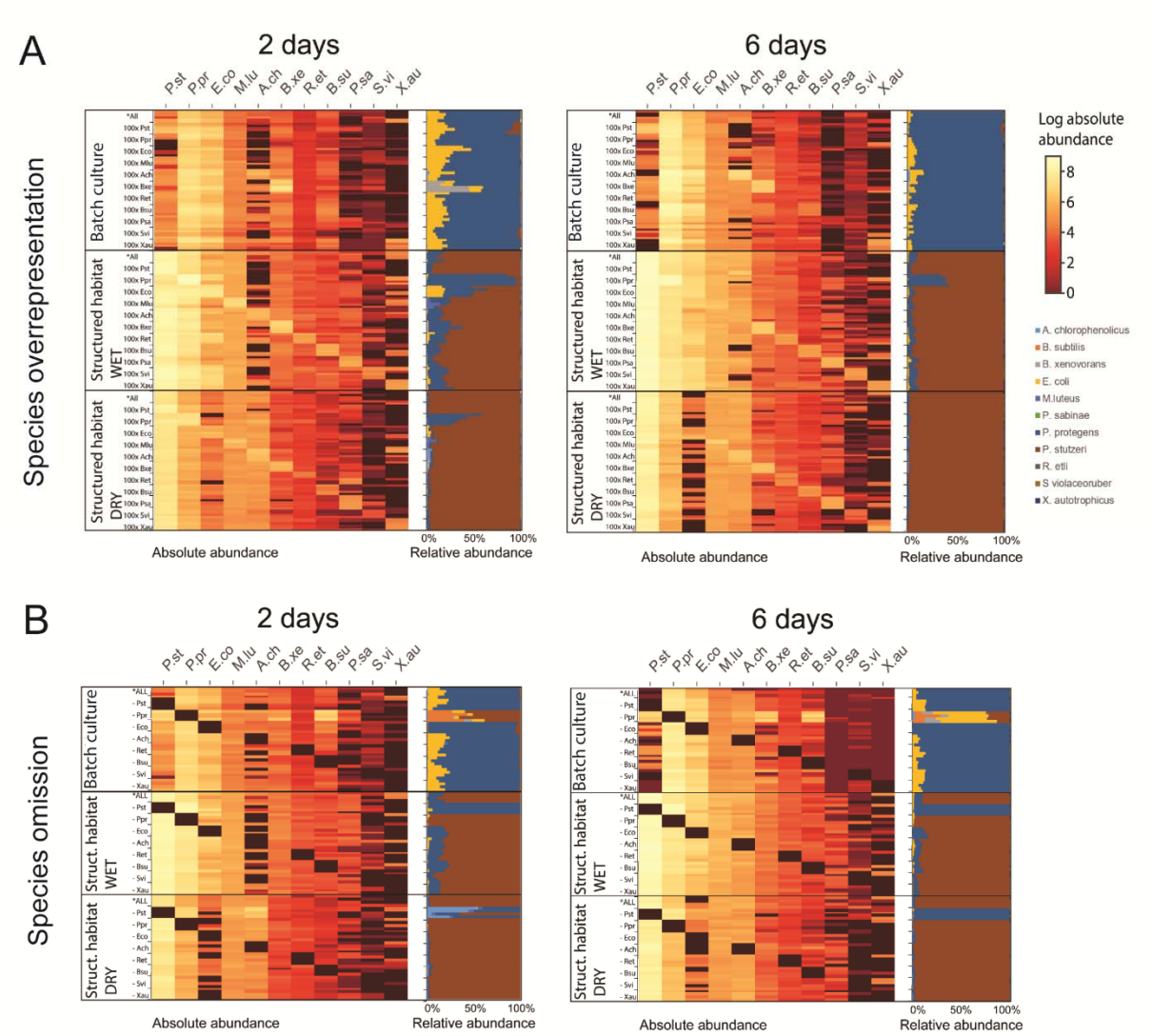

Figure 3. Variations in bacterial community composition in microcosms. The synthetic bacterial community was grown in multi-well plates containing only liquid medium (liquid habitat) or liquid medium mixed with glass beads (spatially structured habitats), the latter with prescribed hydration providing constant wet or relatively dry conditions. Microcosms were sacrificed after 2 or 6 days of incubation for total DNA extraction. Heatmaps show the absolute abundances (log-transformed) of each species (columns) based on the absolute number of genome equivalents measured in each microcosm by qPCR. Absolute counts were used to calculate relative abundance values, shown alongside heatmaps. (A) We investigated the effects of initial species ratios by manipulating the initial composition ratios of the inoculum (100-fold

677 increase of one species at a time compared to the others, 100X…), while a community with
678 even proportions of all species served as a control (*All). The different overrepresented inocula
679 are shown as rows, each with four replicate microcosms per mix. (B) We selected 8 species to
680 be removed from the initial inoculum, thus allowing us to test for causal effects on the growth
681 of the remaining species. The communities are shown as rows, with four replicate microcosms
682 per mix.

683

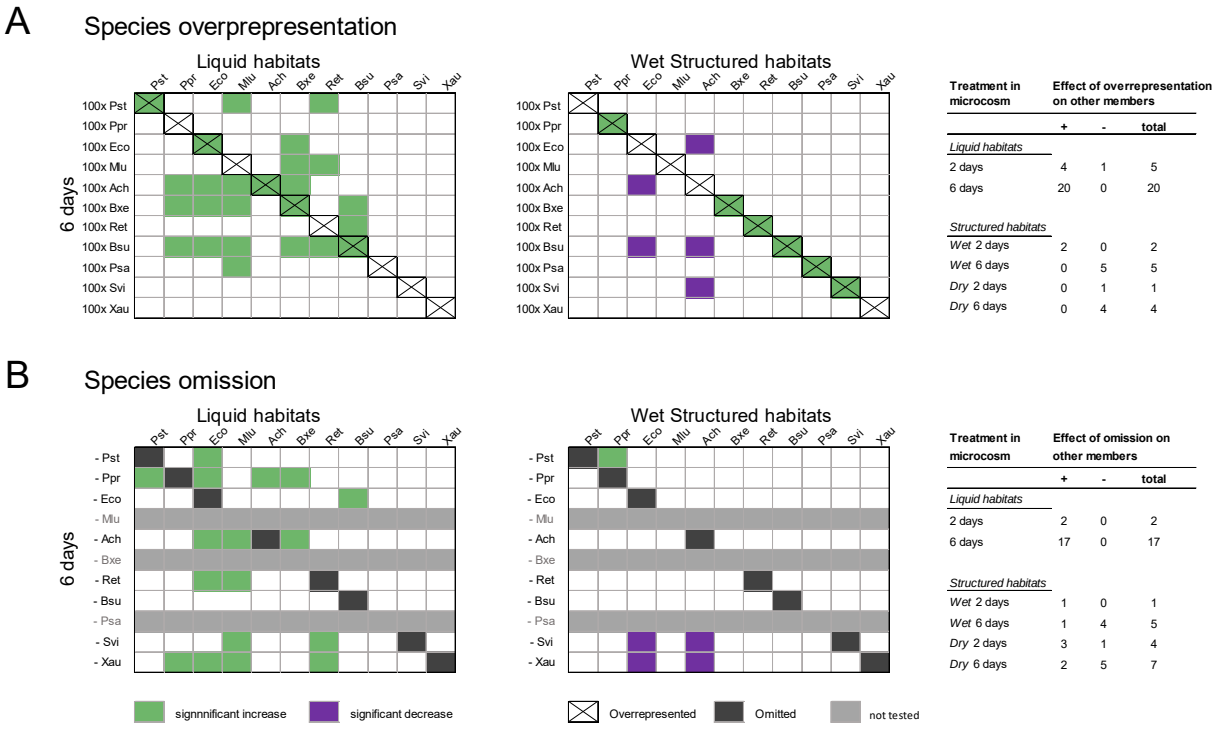

Figure 4. Positive and negative effects of species overrepresentation and omission on other species. Microcosms were inoculated with initial community mixes containing a 100-fold overrepresented species (A) or one omitted species (B). For simplicity we present results from liquid and wet structured habitats after 6 days (full results are shown in Supplementary Fig. S2). Green and magenta colors indicate that the absolute abundance of a given species was respectively significantly higher or lower as a response to overrepresentation or omission of another species in the mix compared to its abundance in control microcosms (inoculated with an even mix of all species, either in liquid or in porous habitats). Variations (increase or decrease) in absolute abundances were deemed significant when >5-fold with a p-value <0.05 (using a two-tailed t-test on 4 replicate microcosms). Tables show the detected effects for all treatments and time points, excluding the effects of a species on itself. A significant increase (+) or decrease (-) of one species as a response to overrepresentation or omission of another is interpreted here as an interaction between the two species, which could be competitive or facilitative depending on the context.

Supplementary Information

Supplementary Methods

Preparation and incubation of microcosms

Structured microcosms were set-up in 96-well plates with a flat 0.22 µm filter membrane at the bottom (Merck, Darmstadt, Germany) containing 250 mg of sterile glass beads (with diameter of 80 to 120 µm) per well. Individual 96-well plates were placed on a layer of quartz flour atop a ceramic plate (1 bar, 12 cm diameter, 0.5 cm thick). The quartz flour ensured a tight connection of the plate's wells with the ceramic -plate. Both the layer of quartz flour and the ceramic plate had been pre-saturated with saline solution (0.9% NaCl) and connected to a medium reservoir containing 800 ml saline solution in a bottle. All parts had been sterilized by autoclaving at 120 °C (saline-solution, medium, glass beads) or alternatively treated at 100 °C for 20 minutes (ceramic disc with heat sensitive glue). The saturated quartz flour and ceramic plate permitted us to maintain a continuous liquid connection between the microcosms and the medium reservoir, and the height of the liquid column served to prescribe hydration conditions in the microcosms. Lowering the reservoir bottle induces drainage of liquid from the microbead habitat by a suction that increases with increasing vertical distance between the bead surface and the liquid level of the medium reservoir. This method allows us to induce unsaturated conditions where the energy level of the water is reduces near particle surface where capillary and adsorptive forces dominate. The matric potential (Ψ_m) describes adhesive intermolecular forces between the water and the solid as negative pressure expressed in –kPa with the equation $\Psi_m = \rho\ g\ h$, where ρ is the density of water, g is the acceleration of gravity, and h is the height of the liquid column (1). Microcosms in this experiment were kept at a fixed hydration level mimicking WET and DRY conditions with a matric potential of – 0.5 kPa and -6 kPa that is ~5 cm and ~60 cm head difference between the microcosm surface and the medium level in the reservoir. Matric potential was allowed to establish and equilibrate for 5 h prior to inoculation.

Two liquid habitat set ups (2 day and 6 day sampling point) and four microbead setups (2 days WET + DRY and 6 days WET + DRY) and were prepared. All multiwall plates harbour 80 parallel microcosms for 20 different microbial communities (one at equal proportions, 11 with one member 100x overrepresented and 8 communities missing one members) and four biological replicates per community. Structured habitats containing 250 mg glass-beads were placed on top of the hydration controlled ceramic. Fast wet up of the glass-beads indicate connectivity of the system. As culture medium 240 µl 0.1x TSBM were added to each microhabitat and bacterial communities were inoculated as described above.

DNA extraction and quantification

For nucleic acid purification the bacterial communities were recovered from the microcosms including the liquid medium or the microbead-matrix and suspended in 180 µl lysis buffer for nucleic acids purification (ATL buffer), to ensure recovery of filamentous growing species a cut tip with enlarged aperture was used. After transfer to 96-rack with 1.2 ml tubes (Brand GmbH + co KG, Wertheim, Germany) the samples were immediately frozen in liquid nitrogen and stored at -80 °C. After the experiment was completed samples were thawed on ice and DNA was extracted using the procedure described in the DNeasy blood and tissue handbook (Qiagen, Hilden, Germany) and the customized additional protocol for increased cell-lysis efficiency through a bead-beating step initiating the extraction procedure provided by the manufacturer. For cell lysis 250 mg glass beads were added to the liquid culture samples (WET and DRY samples already contained the glass bead-matrix) and samples were homogenized in a TissueLyser for 30 s at 6.5 m s−1. DNA was eluted with 50 µl elutions buffer AE to increase DNA yield a second elution step was performed using the 50 µl eluate from the first elution. DNA concentration was quantified fluorometrically using the Qubit dsDNA HS assay kit (Thermo Fischer Scientific) designed specifically to detect double-stranded DNA with high

752 sensitivity in a 384 well plate assay. For readout, we used the Spark 10M Multimode Microplate
753 Reader (Tecan, Männedorf, Schwitzerland) (Fig. S1).
754

755 ## Microfluidic quantitative real-time PCR

756 DNA concentration was normalized to approx. 4 ng/µl with a pipetting robot in a liquid
757 handling station (Brand GmbH + co KG). For the pre-amplification PCR, with 9.6 µl of the
758 community DNA in a total reaction volume of 20 µl containing 200 nM of forward and reverse
759 primers (Supplementary Table S1) in 1x GoTaq G2 Colorless Master Mix (Promega,
760 Duebendorf, Switzerland). Preamplification was performed on a PCR thermal cycler
761 (Sensoquest, Goettingen, Germany) with the following program: initial denaturation at 95°C
762 for 10 min, followed by 15 cycles of denaturation at 95°C for 30 s, annealing at 59°C for 30 s,
763 elongation at 72°C for 90 s, followed by a final elongation step at 72°C for 10 min. Primers
764 were removed prior to reatl-time quantitative PCR by treating 5 µl of the reaction with 10 U
765 Exonuclease I (Thermo Fisher Scientific) at 37 °C for 15 min followed by a heat inactivation
766 step of the enzyme at 85 °C for 15 min. The remaining PCR reaction was amplified for another
767 15 cycles, and the product was further visualized on an agarose gel to control for the presence
768 of a single amplicon with size of ~1.5 kb.
769 The exonuclease-treated PCR products were diluted 5 times in DNA suspension buffer (10 mM
770 Tris, pH 8.0, 0.1 mM EDTA) and 2 µl diluted PCR product were added to 3 µl sample mix
771 containing 1x qPCR Mix (HOT FIREPol EvaGreen qPCR Mix Plus (ROX), Solis Biodyne,
772 Tartu, Estonia) and 1x DNA Binding Dye (Fluidigm Corporation), with a final volume of 5 µl.
773 For the assay mix 1x Assay Loading Reagent (Fluidigm, PN 85000736) was combined with
774 100 µM of forward and reverse primer and nuclease free water was added to a final volume of
775 4 µl (3 µl per inlet plus 1 µl overage). Supplementary Table S1 contains species-specific primer

776 pairs used in the assay. All primers were previously designed and tested for the characterization
777 of our representative soil bacterial community.
778 After mixing 3 µl of the assay and of the sample mix were added to the respective inlet of the
779 192.24 Dynamic Array (Fluidigm) and the chip was loaded and run on the Biomark system
780 using the same real-time quantitative PCR protocol as described previously (2) In total samples
781 from 480 bacterial communities (4 biological replicates) plus 20 community DNA samples used
782 for inoculation were assayed on 3 IFC-chips each designed for 192 samples to be automatically
783 combined with a duplicate set of 12 primer-pairs (Gene Expression 192.24 IFC, Fluidigm corp.)
784 together with two negative controls and an eight point standard calibration in duplicate per chip.
785

Supplementary Figures

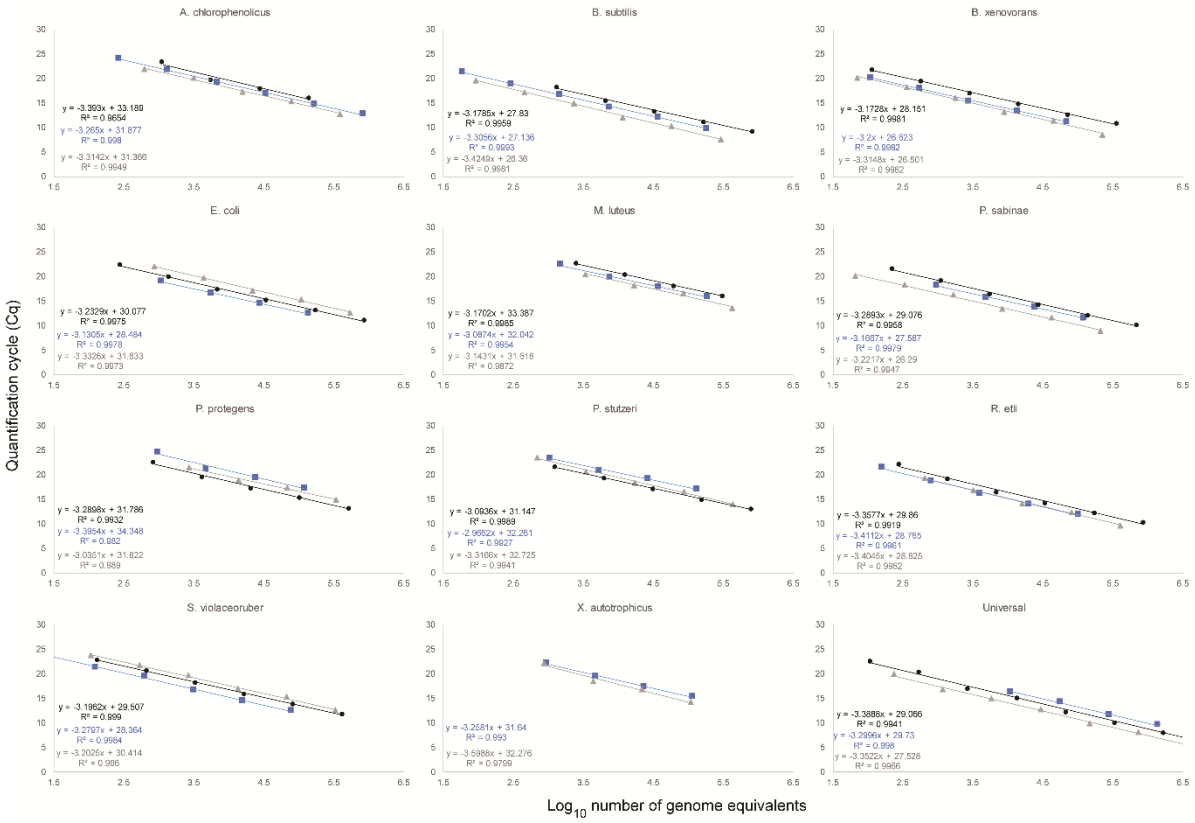

Figure S1. Standard Calibration Curves. Standard calibration curves to calculate abundance of each member of the bacterial community from qPCR data. Purified genomic DNA with known concentration from eleven individual species (Bacterial strains detailed in the Material and Methods section) were combined in equal proportions to prepare fivefold serial dilutions and run in parallel reaction on a Biomark GeneExpression 48.48 IFC (Fluidigm) with each individual species-specific primer pair or with a universal primer pair (Table S1). Based on genome size and known concentration of genomic DNA per species in the stock solution the number of genome equivalent copies was calculated and plotted against the cycle threshold for each species-specific qPCR assay. Data evaluation was performed with the Fluidigm software from four technical replicates per dilution. Standard calibration was calculated for three independent qPCR chips, displayed in black, blue and grey. Equations of fitted linear regression

801 lines and R2 values are shown, calculated from average Cq values. For data evaluation the
802 average values from all three calibrations were used.

803

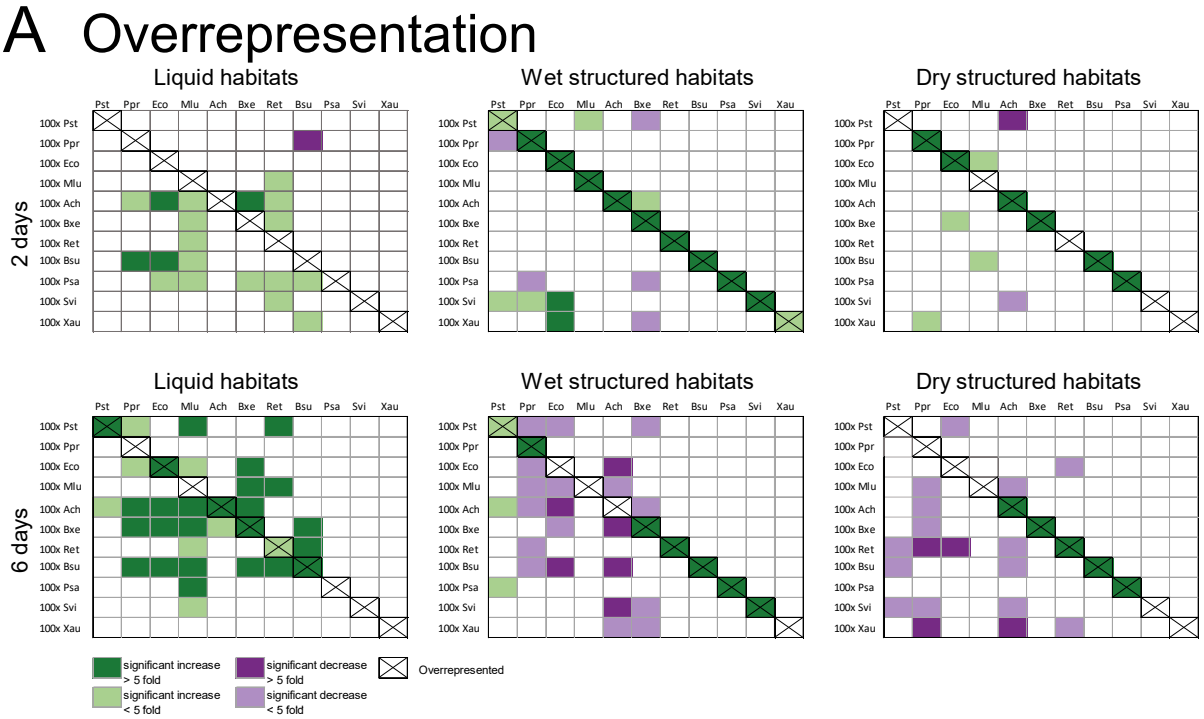

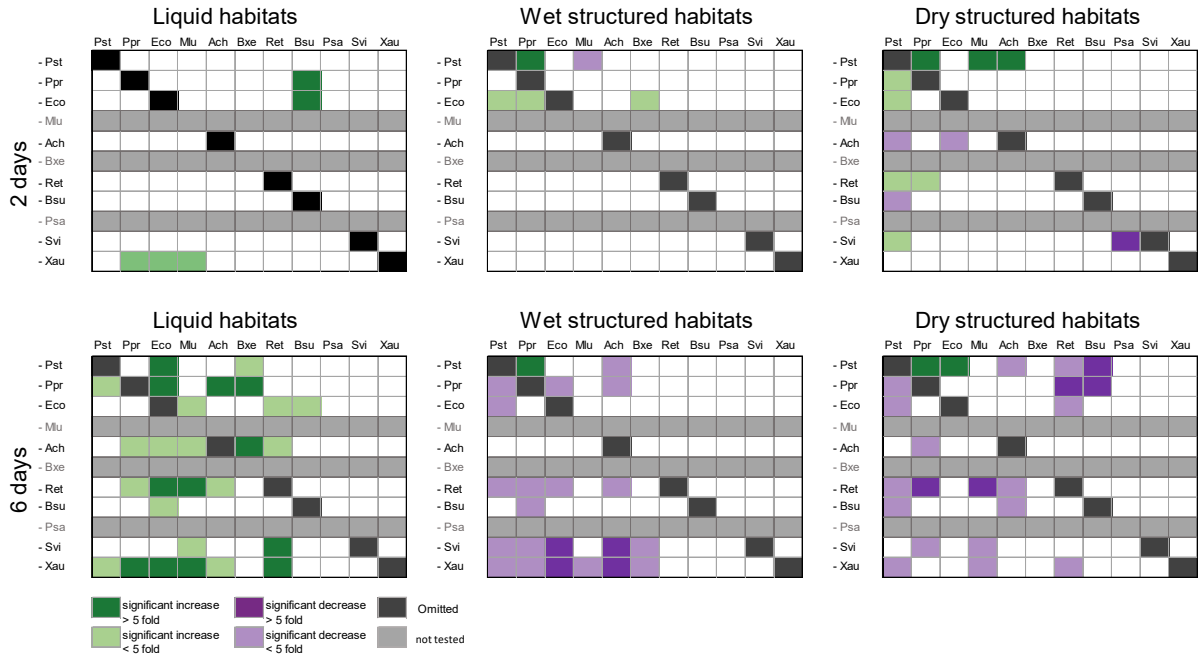

Figure S2. Positive and negative interactions between individual species. (A) Microcosms were inoculated with initial community mixes containing one overrepresented species. (B) Microcosms were inoculated with community mixes where one species has been omitted. This was done for all species except *B. xenovorans*, *M. luteus* and *P. sabinae*. Green and magenta colors indicate that the absolute abundance of a given species was respectively significantly

814 higher or lower compared to the control microcosms (inoculated with an even mix of all
815 species). Variations (increase or decrease) in absolute abundances were deemed significant with
816 a p-value <0.05 (using a two-tailed t-test on 4 replicates) for light colours and significant with
817 an in- decrease of >5-fold dark colours.
818

Supplementary Tables

Table S1. Primers used in real-time PCR.

Name	Sequence (5' to 3')	Tm [°C]	CG Content [%]	Length [nt]	Target pos. 16S	Reference
Species-specific primer pairs						
A_chlo F	CAGCTTGCTGGTGGATTA	60.5	50.0	18	118-283	(2)
A_chlo R	CACCATGCGATGATCAGT	61.3	50.0	18		(2)
B_subt F	GACAGATGGGAGCTTGCT	61.1	55.6	18	82-165	(2)
B_subt R	TGTAAGTGGTAGCCGAAGC	61.0	52.6	19		(2)
B_xeno F	AATACATCGGAACGTGTCCT	61.3	45.0	20	128-209	(2)
B_xeno R	TCCTCTCAGACCAGCTACAG	60.3	55.0	20		(2)
E_coli F	GAAGCTTGCTTCTTTGCTG	61.0	47.4	19	73-177	(2)
E_coli R	TTGGTCTTGCGACGTTATG	62.8	47.4	19		(2)
M_lute F	GACATGTTCCCGATCGCC	67.1	61.1	18	79-183	(2)
M_lute R	CCACCATTACGTGCTGGC	65.7	61.1	18		(2)
P_prot F	GTACTTGTACCTGGTGGCG	61.2	57.9	19	153-270	(2)
P_prot R	GTATTAGCGCCCGTTTCC	62.4	55.6	18		(2)
P_sabi F	GAGTTATGATGGAGCTTGCT	59.0	45.0	20	68-201	(2)
P_sabi R	GGTATGCACCAGAAGGTCTT	61.1	50.0	20		(2)
P_stut F	CTTGCTCCATGATTCAGC	60.1	50.0	18	79-157	(2)
P_stut R	ACGTATGCGGTATTAGCGT	60.2	47.4	19		(2)
R_etli F	GTATACTGTTCGGTGGCG	59.1	55.5	18	781-971	(3)
R_etli R	GAAGGGAACCCTGCATC	60.7	58.8	17		(3)
S_viol F	GAACGATGAACCACTTCGGTG	65.3	50.0	20	64-179	(2)
S_viol R	GATGCCTGCGAGGGTCAGTA	66.2	57.9	19		(2)
X_auto F	GATCTACCCAATGGTACGG	59.5	52.6	19	68-180	(2)
X_auto R	GTTCATCCAATGGCGATA	60.0	44.4	18		(2)
Universal primer pairs						
27F	AGAGTTTGATCCTGGCTCAG	61.5	50	20		(4)
1492R	CGGTTACCTTGTTACGACTT	58.7	45	20		(4)
1099F mod	AACGAGCGCAACCCT	61.2	60	15		modified from (4)
1407R mod	GACGGGCGGTGTGTA	60.9	66.7	15		modified from (5)

823 **Table S2.** Species used in study are well characterized at the genomic and phenotypic level and
824 span a wide diversity of bacterial phyla. Selected species differ in physiology, but all grow
825 aerobically and can be cultivated under standard laboratory conditions.

Species	Phylogeny/Class	Description
Arthrobacter chlorophenolicus (Ach)	Actinobacteria	Soil, rods/cocci, motile, non-spore-forming, involved in bioremediation of phenols such as 4-chlorophenol (4-CP), 4-nitrophenol (4-NP) and phenol [6]
Bacillus subtilis (Bsu)	Firmicutes,	Soil, rods, motile, spore-forming, of industrial relevance due to production of hyaluronic acids, specifically proteases [7, 8]
Burkholderia xenovorans (Bxe)	Betaproteobacteria,	Rhizosphere, rods, motile, non-spore-forming, play important role in bioremediation due to ability to degrade polychlorinated biphenyl (PCB) [9]
Escherichia coli (Eco)	Gammaproteobacteria	Usually found in intestine of warm-blooded organisms, but often detected as faecal contaminant in environmental samples [10, 11], rods, motile, non-spore- forming
Micrococcus luteus (Mlu)	Actinobacteria	Soil cocci, non-motile, non-spore-forming, involve in bioremediation: ability to degrade toxic organic pollutants and tolerance to metals [12]
Paenibacillus sabinae (Psa)	Firmicutes	Rhizosphere, rods, motile, spore-forming, have ability to fix nitrogen [13]
Pseudomonas protegens (Ppr)	Gammaproteobacteria	Rhizosphere, rods, motile, non-spore-forming, have biocontrol properties: plant-protecting bacteria, produces the antimicrobial compounds pyoluteorin and 2,4-diacetylphloroglucinol (DAPG) which are active against various plant pathogens [14]
Pseudomonas stutzeri (Pst)	Gammaproteobacteria	Rhizosphere, rods, motile, non-spore-forming Nitrogen fixation, denitrification, bioremediation due to ability to degrade polycyclic aromatic hydrocarbons (PAHs) [15]
Rhizobium etli (Ret)	Alphaproteobacteria	Rhizosphere, rods, motile, non-spore-forming, form symbiotic relationship with legumes performing nitrogen fixation [16]
Streptomyces violaceoruber (Svi)	Actinobacteria	Soil, filaments, non-motile, spore-forming, model organism for gram-positive soil bacteria of high G+C content that undergoes a complex life cycle of mycelial growth and spore formation and produces a variety of antibiotics and other drugs during the differentiation process [17]
Xanthobacter autotrophicus (Xau)	Alphaproteobacteria	soil, rods, non-motile, non-spore-forming Nitrogen fixation, involved in bioremediation via degradation of 1,2-dichloroethane, methanol and propane [18]

826
827

Supplementary References

1. D. Hillel, Introduction to environmental soil physics (Academic press, 2003).
2. H. Kleyer, R. Tecon, D. Or, Resolving Species Level Changes in a Representative Soil Bacterial Community Using Microfluidic Quantitative PCR. Frontiers in Microbiology 8 (2017).
3. H. Kleyer, R. Tecon, D. Or, Rapid Shifts in Bacterial Community Assembly under Static d Dynamic Hydration Conditions in Porous Media. Appl Environ Microbiol 86 (2019).
4. D. Lane, 16S/23S rRNA sequencing. Nucleic acid techniques in bacterial systematics., 115-175 (1991).
5. S. E. Dyksterhouse et al., Cycloclasticus pugetii gen. nov., sp. nov., an aromatic hydrocarbon-degrading bacterium from marine sediments. 45, 116-123 (1995).
6. Zheng Liu, Chao Yang, Chuanling Qiao, Biodegradation of p-nitrophenol and 4-chlorophenol by Stenotrophomonas sp., FEMS Microbiology Letters, Volume 277, Issue 2, December 2007, Pages 150–156, https://doi.org/10.1111/j.1574-6968.2007.00940.x
7. Widner B, Behr R, Von Dollen S, et al. Hyaluronic acid production in Bacillus subtilis. Appl Environ Microbiol. 2005;71(7):3747-3752. doi:10.1128/AEM.71.7.3747-3752.2005
8. Sze, J.H., Brownlie, J.C. & Love, C.A. Biotechnological production of hyaluronic acid: a mini review. 3 Biotech 6, 67 (2016). https://doi.org/10.1007/s13205-016-0379-9
9. Tehrani R, Lyv MM, Kaveh R, Schnoor JL, Van Aken B. Biodegradation of mono-hydroxylated PCBs by Burkholderia xenovorans. Biotechnol Lett. 2012;34(12):2247-2252. doi:10.1007/s10529-012-1037-x
10. Boehm AB, Wang D, Ercumen A, Shea M, Harris AR, Shanks OC, et al. (2016) Occurrence of Host-Associated Fecal Markers on Child Hands, Household Soil, and Drinking Water in Rural Bangladeshi Households. Environ. Sci. Technol. Lett 3: 393–398.
11. Navab-Daneshmand T, Friedrich MND, Gächter M, et al. Escherichia coli Contamination across Multiple Environmental Compartments (Soil, Hands, Drinking Water, and Handwashing Water) in Urban Harare: Correlations and Risk Factors. Am J Trop Med Hyg. 2018;98(3):803-813. doi:10.4269/ajtmh.17-0521
12. Sandrin TR, Maier RM. Impact of metals on the biodegradation of organic pollutants. Environ Health Perspect. 2003;111(8):1093-1101. doi:10.1289/ehp.5840

13. Ma Y, Xia Z, Liu X, Chen S. Paenibacillus sabinae sp. nov., a nitrogen-fixing species isolated from the rhizosphere soils of shrubs. Int J Syst Evol Microbiol. 2007;57(Pt 1):6-11. doi:10.1099/ijs.0.64519-0
14. J Almario, M Bruto, J Vacheron, C Prigent-Combaret, Y Moënne-Loccoz, D. Müller. Distribution of 2, 4-diacetylphloroglucinol biosynthetic genes among the Pseudomonas spp. reveals unexpected polyphyletism. Frontiers in microbiology 8, 1218
15. Gałązka, Anna, Maria Król, and Andrzej Perzyński. "The efficiency of rhizosphere bioremediation with Azospirillum sp. and Pseudomonas stutzeri in soils freshly contaminated with PAHs and diesel fuel." Polish Journal of Environmental Studies 21.2 (2012).
16. Resendis-Antonio O, Reed JL, Encarnación S, Collado-Vides J, Palsson BØ (2007) Metabolic Reconstruction and Modeling of Nitrogen Fixation in Rhizobium etli. PLoS Comput Biol 3(10): e192. https://doi.org/10.1371/journal.pcbi.0030192
17. Kannika Duangmal, Alan C. Ward, Michael Goodfellow, Selective isolation of members of the Streptomyces violaceoruber clade from soil, FEMS Microbiology Letters, Volume 245, Issue 2, April 2005, Pages 321–327, https://doi.org/10.1016/j.femsle.2005.03.028
18. Parnell JJ, Park J, Denef V, et al. Coping with polychlorinated biphenyl (PCB) toxicity: Physiological and genome-wide responses of Burkholderia xenovorans LB400 to PCB-mediated stress. Appl Environ Microbiol. 2006;72(10):6607-6614. doi:10.1128/AEM.01129-06